

# Learning-Based Rich Feedback HARQ for Energy-Efficient Short Packet Transmission

Martin V. Vejling, *Student Member, IEEE*, Federico Chiariotti, *Member, IEEE*, Anders E. Kalør, *Member, IEEE*, Deniz Gündüz, *Fellow, IEEE*, Gianluigi Liva, *Senior Member, IEEE*, Petar Popovski, *Fellow, IEEE*

## Abstract

The trade-off between reliability, latency, and energy-efficiency is a central problem in communication systems. Advanced hybrid automated repeat request (HARQ) techniques can reduce the number of retransmissions required for reliable communication, but they have a significant computational cost. On the other hand, strict energy constraints apply mainly to devices, while the access point receiving their packets is usually connected to the electrical grid. Therefore, moving the computational complexity required for HARQ schemes from the transmitter to the receiver may provide a way to overcome this trade-off. To achieve this, we propose the Reinforcement-based Adaptive Feedback (RAF) scheme, in which the receiver adaptively learns how much additional redundancy it requires to decode a packet and sends *rich feedback* (i.e., more than a single bit), requesting the coded retransmission of specific symbols. Simulation results show that the RAF scheme achieves a better trade-off between energy-efficiency, reliability, and latency, compared to existing HARQ solutions and a fixed threshold-based policy. Our RAF scheme can easily adapt to different modulation schemes, and since it relies on the posterior probabilities of the codeword symbols at the decoder, it can generalize to different channel statistics.

## Index Terms

Rich feedback, HARQ, Green IoT, short codes.

M. V. Vejling (mvv@es.aau.dk), F. Chiariotti (chiariot@dei.unipd.it, corresponding author), A. E. Kalør (aek@es.aau.dk), and P. Popovski (petarp@es.aau.dk) are with the Dept. of Electronic Systems, Aalborg University, Denmark. F. Chiariotti is also with the Dept. of Information Engineering, University of Padova, Italy. A. E. Kalør is also with the Dept. of Electrical and Electronic Engineering at the University of Hong Kong, Hong Kong. D. Gündüz (d.gunduz@imperial.ac.uk) is with the Dept. of Electrical and Electronic Engineering, Imperial College London, UK. G. Liva (gianluigi.liva@dlr.de) is with the Institute of Communications and Navigation, German Aerospace Center (DLR), Wessling, Germany.

This work was partly funded by the Villum Investigator Grant “WATER” financed by the Villum Foundation, Denmark. The work of F. Chiariotti was financed by the European Union under the Italian National Recovery and Resilience Plan of NextGenerationEU, under the “SoE Young Researchers” grant REDIAL (SoE0000009). The work of A. E. Kalør was supported by the Independent Research Fund Denmark (IRFD) under Grant 1056-00006B.

## I. INTRODUCTION

Over the past few years, Internet of Things (IoT) systems have become ubiquitous [1]: factories, buildings, farms, and urban environments now have extensive networks of simple IoT devices, which can collect all sorts of data, improving energy-efficiency and informing economic and policy decisions [2]. Most IoT devices have extremely long design lifespans, often measured in years or decades [3], and the main limitation they face is the energy consumption, as replacing batteries is an expensive operation in many cases. For this reason, several low-energy protocols have been developed [4], and energy-efficiency is a significant concern in IoT research.

Some critical applications, such as industrial and environmental monitoring, require relatively high reliability. To achieve this, IoT devices need to either increase their transmission power, consuming more of their limited battery, or use hybrid automated repeat request (HARQ) [5], an extension of the simple retransmission model, in which the transmitter adds some redundant information in each retransmission, while the receiver combines the previously received information with the new transmission to decode the original message. As such, HARQ solves the rate selection problem in communication protocols with reliability constraints by dynamically adapting the rate to the state of the decoder. The energy consumption of HARQ can be reduced by adapting the transmit power to achieve the required reliability while minimizing the total expected energy consumption [6]. However, this may come at the expense of increased latency, as the first transmission attempts are often allocated lower power to save energy.

Overall there is a fundamental trade-off between reliability, latency, and energy consumption [7]: (i) a low-rate code in the first transmission leads to fewer rounds of HARQ, and hence a lower latency, but requires more energy as well; (ii) retransmitting fewer symbols in each round leads to higher latency and lower reliability, but is more energy-efficient, as the IoT device transmits the exact number of symbols needed to decode the packet. On the other hand, multiple rounds of feedback can also lead to a high energy consumption, as the reception of the feedback may require almost as much energy as active transmission [8], and needs to be taken into account. Computation is another aspect that cannot be neglected [9]: complex schemes that put a significant computational load on the transmitter side can deplete batteries just as quickly as inefficient transmission.

### A. Related Work

The dominant form of HARQ schemes in practical systems relies on a single feedback bit conveying success (ACK) or failure (NACK), while the size of the retransmitted packet is fixed in advance, such as those employed in narrowband IoT (NB-IoT) [10]. Techniques for sequential differential optimization (SDO) optimize throughput by minimizing the average number of symbol transmissions [11] in the case of single bit feedback, and recently an SDO procedure for variable-length stop-feedback codes has been developed, computing optimal decoding times for binary-input additive white Gaussian noise (AWGN) channels [12]. However, this cannot readily generalize to more complex channels.

It is also possible to transmit more complex information, such as the full channel state information (CSI) or the accumulated mutual information, allowing the transmitter to make informed decisions and adapt to the instantaneous channel state. Code-adaptive HARQ techniques [13] optimize the encoding and modulation of retransmitted packets, exploiting the additional information from the rich feedback to improve HARQ energy-efficiency even if the feedback is outdated or inaccurate [14], at the cost of significant computational load on the transmitter. Recently, a rich feedback protocol was proposed [15], which uses the decoded message as feedback and a compressed error vector in the retransmissions. This allows the transmitter to maximize the probability of decoding in each round and yields a trade-off between spectral efficiency, reliability, and latency. However, the feedback contains the same number of bits as the transmission, potentially leading the transmitter to spend a significant amount of energy for reception. In another recent work [16], a feedback based variable-length transmission scheme for convolution codes and turbo codes has been proposed: the scheme relies on instantaneous feedback to opportunistically adapt the symbol length to the noise realization within a sub-symbol interval.

While traditional feedback codes relying on rich feedback suffer from quantization constraints, deep learning-based feedback codes can be trained to alleviate these costs [17]. In [18], a code based on the transformer architecture is designed to address some of the issues with deep learning based feedback codes: reducing the communication overhead introduced by feedback rounds and allowing for flexible rate selection. In another recent work, a rateless autoencoder coding scheme is proposed to trade-off reliability and latency [19]. Although these codes have proven to be effective for feedback based communications, the energy consumption, caused by the complex

operations at the transmitter, is significant in the context of energy-constrained devices.

### *B. Contributions and Organization*

In this paper, we consider a battery-powered transmitter that needs to perform energy-efficient HARQ, minimizing its total energy consumption while maintaining a relatively low latency. The receiver does not have the same energy limitations, therefore it can perform more complex operations and send rich feedback to conserve the transmitter's battery. This requires a scheme that enjoys the benefits of adaptive HARQ while shifting the energy cost toward the receiver as much as possible.

We consider the transmission of short packets encoded using non-binary low-density parity check (LDPC) codes [20], which proved to be highly efficient in the short block length regime [21]. Transmission of short packets is common in robotic control and IoT. We employ a class of rate-compatible codes known as multiplicatively repeated (MR) non-binary LDPC codes [22], where additional redundancy symbols can be obtained by multiplying codeword symbols (*multiplicative repetitions*) by a nonzero field element. We then model the feedback design problem as a Markov decision process (MDP) and propose the Reinforcement-based Adaptive Feedback (RAF) scheme, in which the receiver can specify which symbols should be retransmitted, optimizing the trade-off between the latency and energy cost of transmission while guaranteeing high reliability. This decision is adaptive and dynamic, as it is based on the state of the message passing decoder and not just on the measured signal to noise ratio (SNR), and allows for a faster, more efficient HARQ protocol.

The main contributions of this paper can be summarized as follows:

- 1) We propose RAF, a rich feedback HARQ scheme, which can improve the energy efficiency-latency trade-off for short-packet transmissions by learning the optimal feedback policy using reinforcement learning (RL) techniques. The novelty of this scheme is the design of the feedback based on the state of the decoder.
- 2) The proposed scheme is compared to existing HARQ solutions and a fixed threshold-based policy in the context of MR non-binary LDPC codes with different modulation schemes and channels.
- 3) Trade-off between the energy-efficiency, latency, and reliability is addressed for a state of the art energy model.

Our simulations show that RAF outperforms the traditional HARQ and the fixed threshold-based policies by improving all key performance indicators (KPIs) at once. Specifically, compared to HARQ, we are able to reduce the undetected error rate by one third, while latency and energy efficiency are slightly improved with respect to the optimized benchmarks. Moreover, RAF can readily generalize to different modulation schemes and channels.

The rest of this paper is organized as follows. Sec. II describes the basic communication model, the rich feedback HARQ scheme, and the energy model, while the MDP problem formulation and the proposed RAF scheme are presented in Sec. III. Numerical results are presented in Sec. IV, and Sec. V concludes the paper and presents some future research directions.

## II. SYSTEM MODEL

We consider an energy-constrained device that needs to reliably transmit a message  $m \in \{0, 1, \dots, 2^K - 1\}$  of  $K$  bits over a wireless channel with the minimum possible energy expenditure. The receiver has unlimited energy resources and computational capabilities. The message is transmitted over a variable number of *transmission rounds* indexed by  $t = 0, 1, \dots, T_{\max} - 1$ , comprising a variable number of uplink channel uses (or channel symbols) followed by a fixed number of downlink channel uses for feedback. The number of uplink channel uses in round  $t$  is denoted by  $\hat{L}_t$  and determined by the number of transmitted codeword symbols  $L_t$  (also variable) and the number of channel uses per codeword symbol (assumed to be constant). Assuming an  $M$ -ary quadrature amplitude modulation (QAM) scheme and that the codewords are defined over the order- $q$  Galois field (GF)  $\mathbb{F}_q$ , the number of uplink channel uses in the  $t$ -th round is given by  $\hat{L}_t = \frac{\log_2(q)}{\log_2(M)} L_t$ . The rate of communication after the  $t$ -th round is thus  $R_t \triangleq K / (\sum_{i=0}^t \hat{L}_i)$  bits per channel use. Throughout the paper, we will assume that  $q \leq M$  so that each codeword symbol produces  $\frac{\log_2(q)}{\log_2(M)} \geq 1$  channel symbols, but the general framework can be applied to the alternative case as well. The transmission terminates when the message has been decoded by the receiver (elaborated in Sec. II-B) or with failure after  $T_{\max}$  rounds.

We assume that the energy-constrained device transmits a fixed number  $L_0$  of codeword symbols in the first round, and at most  $L_0$  symbols in each of the following rounds, i.e.,  $L_t \leq L_0$ ,  $t = 1, \dots, T_{\max} - 1$ . Furthermore, we assume that the same modulation scheme is used for the downlink, and denote the number of downlink channel uses in each frame by  $\hat{L}_f = \frac{\log_2(q)}{\log_2(M)} L_f$  where  $L_f$  is the number of feedback symbols. Contrary to the uplink transmission, the feedback

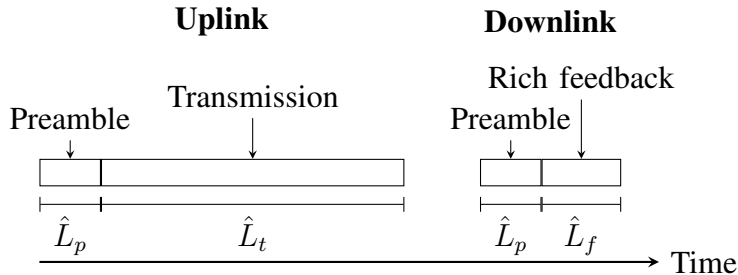


Fig. 1. Communication protocol for the  $t$ -th round.

is received without errors. This can be justified by the fact that the edge node has unlimited power, and thus can transmit with much higher power.

We denote the vector of complex uplink channel symbols in round  $t$  by  $\mathbf{x}_t = (x_{t,1}, \dots, x_{t,\hat{L}_t}) \in \mathbb{C}^{\hat{L}_t}$ . The channel symbols are assumed to have normalized average power, i.e.,  $\mathbb{E}[|x_{t,i}|^2] = 1$  for  $i = 1, \dots, \hat{L}_t$ , and are transmitted over a block fading channel so that the signal received by in round  $t$ , denoted  $\mathbf{y}_t \in \mathbb{C}^{\hat{L}_t}$ , is

$$\mathbf{y}_t = \beta_t \mathbf{x}_t + \mathbf{w}_t, \quad (1)$$

where  $\beta_t$  is the instantaneous fading coefficient, and  $\mathbf{w}_t \sim \mathcal{CN}(\mathbf{0}, \sigma^2 \mathbf{I})$  is AWGN. Assuming unit bandwidth, the instantaneous SNR is then  $\text{SNR}_t \triangleq \frac{|\beta_t|^2}{\sigma^2}$ .

We will assume that the receiver performs perfect channel estimation. To facilitate this, we assume that each frame (both uplink and downlink) contains a preamble of  $\hat{L}_p = \frac{\log_2(q)}{\log_2(M)} L_p$ ,  $L_p \geq 0$ , channel uses prepended to the data channel uses, as depicted in Fig. 1. Note that by including a preamble in each communication round the protocol becomes robust to channels with a coherence time that is shorter than the time between transmission rounds, which can be the case, for instance, in unlicensed bands with duty-cycle limits, or in protocols with frequency hopping.

### A. MR Non-Binary LDPC Codes

The transmitter employs MR non-binary LDPC codes [22], defined over  $\mathbb{F}_q$ , which allows the device to generate codes with successively lower rates by concatenating previous codewords with a new set of symbols. Specifically, consider a non-binary LDPC code,  $\mathcal{C}$ , with codeword length  $L_0$  and code rate  $K/(L_0 \log_2(q))$ , defined by the null space of a sparse parity check matrix  $\mathbf{H} \in \mathbb{F}_q^{Q \times L_0}$ ,  $Q = K/\log_2 q$ , i.e.,

$$\mathcal{C} = \{\mathbf{c} = (s_1, \dots, s_{L_0}) \in \mathbb{F}_q^{L_0} \mid \mathbf{H}\mathbf{c}^T = \mathbf{0} \in \mathbb{F}_q^Q\}. \quad (2)$$

Using MR with  $\mathcal{C}$  as the mother code, we construct a code  $\mathcal{C}_1$  with rate  $K/(2L_0 \log_2(q)) = Q/(2L_0)$  as

$$\mathcal{C}_1 = \{(s_1, \dots, s_{2L_0}) \in \mathbb{F}_q^{2L_0} \mid s_{L_0+v} = z_{L_0+v} s_v \text{ for } v = 1, \dots, L_0, (s_1, \dots, s_{L_0}) \in \mathcal{C}\}, \quad (3)$$

where  $z_{L_0+v} \sim \text{Uniform}(\mathbb{F}_q \setminus \{0\})$ ,  $v = 1, \dots, L_0$ . Recursively, additional codes  $\mathcal{C}_2, \mathcal{C}_3, \dots$  of rates  $Q/(3L_0), Q/(4L_0), \dots$ , respectively, can be constructed by generating an additional  $L_0$  codewords through MR with  $\mathcal{C}$  as the mother code and concatenating to the previous code. The codewords in  $\mathcal{C}_m$  obtained through this construction still forms a valid linear code and can be viewed as a random non-binary LDPC code over an order- $q$  GF of length  $\log_2(q)(m+1)$  bits.

Adaptive rates can be achieved by puncturing symbols in the MR, for instance, given a puncture pattern  $\mathbf{f}_1 \in \{0, 1\}^{L_0}$ , the index set of MR symbols is  $\mathcal{V}^{\mathbf{f}_1} = \{j \mid j = \sum_{k=1}^i \mathbf{f}_1(k), i \in \{1, \dots, L_0\}, \mathbf{f}_1(i) = 1\}$ , and we can construct a code as

$$\mathcal{C}_1^{\mathbf{f}_1} = \{(s_1, \dots, s_{L_0+L_1}) \in \mathbb{F}_q^{L_0+L_1} \mid s_{L_0+v} = z_{L_0+v} s_v \text{ for } v \in \mathcal{V}^{\mathbf{f}_1}, (s_1, \dots, s_{L_0}) \in \mathcal{C}\}, \quad (4)$$

where  $L_1 = \sum_{i=1}^{L_0} \mathbf{f}_1(i) \leq L_0$ . The rate of this code is then  $Q/(L_0 + L_1)$ . Recursively, codes with rates  $Q/(\sum_{i=0}^t L_i)$ ,  $L_i \leq L_0$ , can be constructed.

## B. HARQ Scheme

We apply these codes to our system as follows. In the first round,  $t = 0$ , message  $m$  is encoded using the mother code into an initial codeword  $\mathbf{c} \in \mathcal{C}_0$  of  $L_0$  code symbols, which the device maps into  $\hat{L}_0$  channel symbols and transmits to the edge node along with the preamble. In each of the following rounds,  $t = 1, 2, \dots, T_{\max} - 1$ , the transmitter constructs *additional*  $L_0$  codeword symbols using the procedure outlined above, and then punctures them to  $L_t \leq L_0$  symbols, which it then transmits along with the preamble, as shown in Fig. 1. This continues until either the receiver is able to decode the message and the device receives an ACK feedback, or  $T_{\max}$  rounds are completed.

The decoder employs belief propagation (BP) decoding with a maximum of  $I$  BP iterations to obtain an estimate  $\hat{\mathbf{c}}_t$  of the initial codeword  $\mathbf{c}$  based on the received signals  $\mathbf{y}_0, \dots, \mathbf{y}_t$ . For details on the BP decoder, the reader is referred to [22]. If  $\hat{\mathbf{c}}_t$  is a valid codeword, i.e.,  $\hat{\mathbf{c}}_t \in \mathcal{C}$ , the message is assumed to be correctly received and the edge node terminates the transmission by sending an ACK. On the other hand, if  $\hat{\mathbf{c}}_t$  is not a valid codeword, then the edge node transmits

a feedback signal (unless  $t = T_{\max} - 1$ , in which case the transmission is abandoned and the packet is dropped).

As discussed in Sec. I-A, there are many ways in which the feedback signal can be designed, such as sending a NACK, corresponding to the binary HARQ, sending CSI, etc. In this work, we propose to design the feedback signal in round  $t - 1$  as the specific puncturing pattern to be used in round  $t$ . The aim of this paper is to learn an adaptive puncturing policy based on the information available at the decoder.

### C. Energy Model

Our central performance metrics are the number of successful information bits transmitted per energy unit consumed by the transmitter, and the latency. To this end, we assume that, on average, transmitting and receiving a single symbol require powers  $P_s$  and  $P_f$ , respectively. The precise values of  $P_s$  and  $P_f$  depend on the physical implementation of the communication system and encompasses energy consumption of active radio frequency (RF) chains as well as encoding and decoding operations. To control the relative cost of receiving and transmitting, we parameterize  $P_f = \alpha P_s$ , where  $\alpha \in [0, 1]$  is the control parameter (we assume that  $P_f \leq P_s$ , as in most practical systems). If  $\alpha = 1$  the costs of receiving and transmitting a symbol are the same, whereas  $\alpha = 0$  corresponds to the case where the receive energy cost is ignored. With this in mind, the average total energy spent by the device in the  $t$ -th round is

$$E(t) = P_s(\hat{L}_p + \hat{L}_t) + \alpha P_s(\hat{L}_p + \hat{L}_f), \quad (5)$$

and the average cumulative energy consumed up until and including the  $t$ -th round is accordingly  $E_{\text{tot}}(t) = \sum_{i=0}^t E(i)$ . We further denote the number of successful information bits transmitted per energy unit consumed by the transmitter as

$$E_b(t) = \frac{K}{E_{\text{tot}}(t)} \mathbb{1}[\hat{\mathbf{c}}_t = \mathbf{c}], \quad (6)$$

where  $\mathbb{1}[\cdot]$  is the indicator function, equal to 1 if the condition is true, and 0 otherwise.

## III. LEARNING-BASED ADAPTIVE FEEDBACK

In this section, we present our proposed adaptive feedback scheme. We first introduce the general feedback design, and then show how to learn the feedback policy using RL.

We propose to control the transmissions by providing a puncturing pattern in the feedback link. Specifically, in round  $t$ , we provide  $\mathbf{f}_{t+1} = (f_{t+1,1}, \dots, f_{t+1,L_0}) \in \{0, 1\}^{L_0}$ , indicating the



binary puncturing pattern that should be used for the uplink transmission in round  $t+1$ , such that the  $j$ -th MR codeword symbol from the mother code  $\mathcal{C}$  is punctured if  $f_{t+1,j} = 0$ . As a result, the uncoded feedback message has length  $L_0$ , and consequently  $L_f = \lceil \frac{L_0}{\log_2 q} \rceil$ <sup>1</sup>. Furthermore, the uplink transmission in round  $t+1$  has length  $L_{t+1} = \sum_{j=1}^{L_0} \mathbf{f}_{t+1,j}$ . Accordingly, an ACK corresponds to the transmission of the puncturing pattern  $\mathbf{f}_{t+1} = \mathbf{0}$ .

The objective is to learn a policy that uses the information from previous rounds to choose the optimal puncturing pattern. At time  $t$ , the information observed at the edge node are the received signals  $\mathbf{y}_0, \dots, \mathbf{y}_t$  and as such we seek a sequence of mappings  $(\mathbf{y}_0, \dots, \mathbf{y}_t) \xrightarrow{\mathcal{F}_t} \mathbf{f}_{t+1}$  for  $t = 0, \dots, T_{\max} - 1$ . This sequence of mappings should be designed to be both energy-efficient and with low latency and we define our overall problem through the coupled optimization problems

$$\mathcal{F}_t^* = \arg \max_{\mathcal{F}_t: \mathbb{C}^{\dot{L}_t \times (t+1)} \rightarrow \{0,1\}^{L_0}} \mathbb{E}_{\mathcal{F}} [E_b(T)\gamma^T], \quad (7)$$

for  $t = 0, \dots, T_{\max} - 1$ , where  $\mathbb{E}_{\mathcal{F}}$  is the expected value operator given that the agent follows policy  $\mathcal{F}_t$  at time  $t$ ,  $T$  is the random variable defining the total number of transmission rounds until termination, and  $\gamma \in (0, 1]$  is an exponential discount factor that is meant to ensure low latency (lower values of  $\gamma$  lead the system to prioritize latency over energy-efficiency). The expectation in Eq. (7) is over  $\mathbf{c}$ , generated from encoding a message  $m$  drawn uniformly from the set of messages, and the time until the transmission terminates,  $T$ , which, given the sequence of mappings  $\mathcal{F}_t$  and  $\mathbf{c}$ , depends only on the channel realizations.

Solving this optimization problem is not straightforward, which motivates a number of simplifications. Firstly, using the received signals as the inputs to the mapping leads to the need for an entire sequence of mappings. This can be overcome by using a sufficient statistic instead, combining the information from all the past rounds. Specifically, we do this by considering the a posteriori probabilities estimated by the BP decoder in each round, denoted by the matrix  $\mathbf{P}_t = [\Pr(s_i = \zeta_j | \mathbf{y}_t, \dots, \mathbf{y}_0)]_{ij}$  where  $\zeta_j$  is the  $j$ -th element in the GF  $\mathbb{F}_q$ . We make an additional simplification to only consider the a posteriori entropy vector,  $\mathbf{h}_t \in \mathcal{S} = [0, \log_2 q]^{L_0}$ , of the codeword symbols  $s_i$ ,  $i = 1, 2, \dots, L_0$ , of the mother code  $\mathcal{C}$ , defined as

$$\mathbf{h}_t(i) = - \sum_{\zeta \in \mathbb{F}_q} \Pr(s_i = \zeta | \mathbf{y}_t, \dots, \mathbf{y}_0) \log_2 \Pr(s_i = \zeta | \mathbf{y}_t, \dots, \mathbf{y}_0). \quad (8)$$

<sup>1</sup>For simplicity, we assume no encoding or compression of the puncturing pattern, noting that the flexibility in the energy model keeps the presentation general.

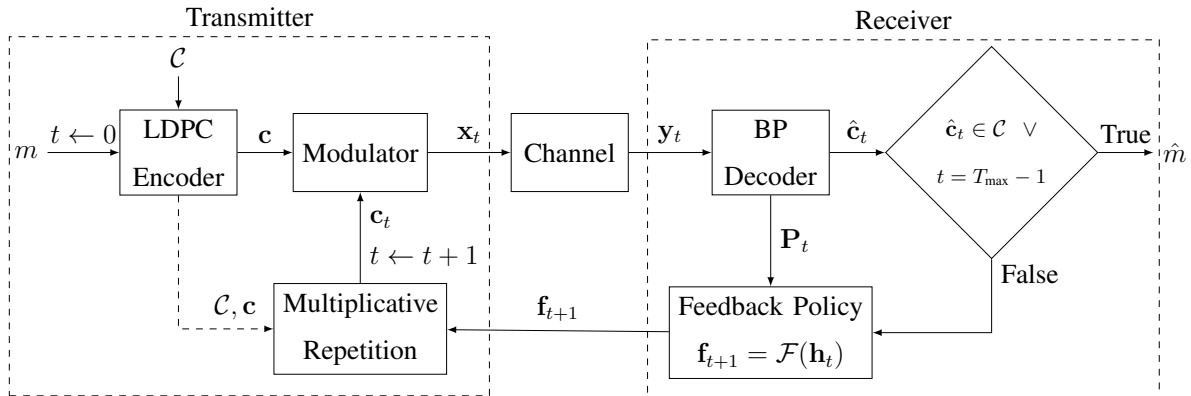


Fig. 2. Block diagram of the proposed rich feedback communication protocol, RAF.

The choice of using  $\mathbf{h}_t$  as the state, as opposed to the full codeword symbol probability matrix  $\mathbf{P}_t$ , is justified by empirical results indicating that using  $\mathbf{P}_t$  does not lead to improvements in the results. The feedback message in round  $t$  is then constructed as  $\mathbf{f}_{t+1} = \mathcal{F}(\mathbf{h}_t)$ , where  $\mathcal{F} : \mathcal{S} \rightarrow \{0, 1\}^{L_0}$  is a deterministic function that maps the entropy vector to a message of  $L_0$  bits indicating the puncturing pattern to be used in round  $t + 1$ . We formulate the simplified objective as

$$\mathcal{F}^* = \arg \max_{\mathcal{F} : \mathcal{S} \rightarrow \{0, 1\}^{L_0}} \mathbb{E}_{\mathcal{F}} [E_b(T) \gamma^T]. \quad (9)$$

To keep the problem tractable and the resulting policy simple, we restrict our attention to stationary, deterministic policies.

The proposed rich feedback communication protocol is summarized in Fig. 2. Note that the proposed feedback is significantly richer than a binary HARQ feedback, which is a single bit requesting the transmission of additional codeword symbols according to some pre-defined scheme known to both the transmitter and the receiver.

### A. MDP Formulation

The problem introduced in Eq. (9) is approximated by an MDP assuming that the next entropy vector is approximately independent of the past given the chosen action and the current entropy

vector.<sup>2</sup> This assumption allows us to characterise the statistics of the system using only one-step dynamics.

The feedback adaptation problem is formulated as a finite-horizon MDP, in which the objective is to maximize  $\mathbb{E}_{\mathcal{F}}[E_b(T)\gamma^T]$  by repeatedly applying  $\mathcal{F}$  to the current state, i.e., the entropy vector  $\mathbf{h}_t$  defined in Eq. (8). Each episode of the MDP corresponds to a message transmission, beginning with the transmission of  $\mathbf{x}_0$  and lasting until the decoder outputs a valid codeword or  $T_{\max}$  (re)transmissions have been reached.

The MDP is defined by the state and action sets, and the one-step dynamics through the conditional density

$$p(\mathbf{h}', r|\mathbf{h}, a) = \Pr(\mathbf{h}_{t+1} = \mathbf{h}', r_t = r|\mathbf{h}_t = \mathbf{h}, a_t = a),$$

where  $\mathbf{h}_t$  is the current state,  $a_t$  is the chosen action,  $\mathbf{h}_{t+1}$  is the state reached in the next round, and finally  $r_t$  is the reward assigned to the chosen action. To solve the MDP problem, RL techniques, such as policy evaluation, policy iteration, value iteration, Q-learning, etc., can be adopted [23]. In this work, we consider Q-learning with the purpose of exploiting the well-known deep Q-network (DQN) approach [24].

Due to the episodic nature of the MDP, we choose to set  $r_t = 0$  for  $t = 1, \dots, T - 1$ , and only assign non-zero rewards at the end of an episode. While  $E_b(T)$  would be a natural choice for rewards following the overall problem defined in Eq. (9), we have chosen a different strategy, since we empirically found faster convergence and more robust training across simulation settings. The reward assignment is based on an additive penalty to energy expenditure. We begin by considering Eq. (5) and defining

$$E_o = P_s \hat{L}_p + \alpha P_s \hat{L}_p + \alpha P_s \hat{L}_f, \quad (10)$$

which is the energy spent on overhead in each communication round. In a scenario with a given latency prioritization, the ratio between  $P_s$  and  $E_o$  defines how “aggressive” the scheme is. The “aggressiveness” of a policy refers to how much additional redundancy the scheme requests in

<sup>2</sup>This is only an approximation since the posterior probabilities do not exactly satisfy the Markov property even though the channel realizations are independent. For an RL algorithm to be successful, it is important that the state is a good basis for predicting future rewards, and usually as the state approaches the Markov property the performance of the RL algorithm improves.

each retransmission (an “aggressive” policy will select a puncturing pattern with a large number of symbols for retransmission). We then define the reward as:

$$r_T = (2 \cdot \mathbb{1}[\hat{\mathbf{c}}_T = \mathbf{c}] - 1) - \frac{E_{\text{tot}}(T)}{\mathbb{E}_{\mathcal{F}_0}[E_{\text{tot}}(T)]}, \quad (11)$$

where  $\mathcal{F}_0$  is a baseline hand-designed policy. In this paper,  $\mathcal{F}_0$  is designed as a naïve static policy which performs poorly (the specific choice is given in Sec. IV). The normalization according to a baseline policy is included since improvements in convergence of the learning algorithm were observed in preliminary results. Although this normalization should only influence the weight assigned to undetected errors relative to energy expenditure, for deep RL it has also been found to have implications on the exploration-exploitation trade-off [25]. In this sense, we employ this normalization to encourage exploring new actions when presented with a state, from which the agent’s actions have previously resulted in poor rewards relative to the baseline policy. Note that, since episodes are finite-horizon and the reward is bounded and non-zero only in the last step of each episode, all policies yield finite expected rewards as well.

The number of actions in the proposed MDP is  $2^{L_0}$ , which is large even for relatively small values of  $L_0$ . The method used in this work to solve the MDP struggles with scalability to high dimensional action spaces, and thus we simplify the action space by instead selecting the *number* of symbols to be retransmitted in the next round. We denote this policy as  $\tilde{\mathcal{F}} : \mathcal{S} \rightarrow \mathcal{A}$ , where  $\mathcal{A} = \{1, \dots, L_0\}$  is the action space of the MDP problem (the action of requesting zero symbols is selected automatically if  $\hat{\mathbf{c}}_t \in \mathcal{C}$ ). Symbols are then requested deterministically according to a policy  $\mathcal{G} : \mathcal{A} \times \mathcal{S} \rightarrow \{0, 1\}^{L_0}$ . This symbol selection policy is defined as requesting the symbols with the highest entropy based on Eq. (8), i.e.,

$$[\mathcal{G}(a_t, \mathbf{h}_t)]_i = \mathbb{1}\left[\sum_{j \neq i} \mathbb{1}[\mathbf{h}_t(i) < \mathbf{h}_t(j)] < a_t\right], \quad (12)$$

where  $a_t \in \mathcal{A}$ . The simplification above is justified by empirical results that suggest optimizing an agent to select which symbols to retransmit yields no performance gains compared to selecting the maximum entropy symbols. With this structure, the composite policy is given as

$$\mathcal{F}(\mathbf{h}_t) = \mathcal{G}(\tilde{\mathcal{F}}(\mathbf{h}_t), \mathbf{h}_t), \quad (13)$$

and the final MDP problem is defined as finding a policy  $\tilde{\mathcal{F}}^*$  that solves

$$\tilde{\mathcal{F}}^* = \arg \max_{\tilde{\mathcal{F}}: \mathcal{S} \rightarrow \mathcal{A}} \mathbb{E}_{\mathcal{F}} [r_T \gamma^T]. \quad (14)$$

Hence, the MDP is now fully specified by the state set,  $\mathcal{S}$ , containing the a posteriori entropy vectors, the action set,  $\mathcal{A}$ , consisting of the actions of choosing the *number* of symbols to be retransmitted, and the reward function specified in Eq. (11).

As mentioned earlier, we will use Q-learning to solve this MDP. Let us consider the expected reward of taking action  $a$  in state  $\mathbf{h}$  at time step  $t$ , and then following the policy  $\mathcal{F}$  in time steps  $t + 1, \dots, T - 1$ :

$$V_{\mathcal{F}}(\mathbf{h}, a) = \mathbb{E}_{\mathcal{F}}[r_T \gamma^{T-t-1} | \mathbf{h}_t = \mathbf{h}, a_t = a]. \quad (15)$$

In Q-learning, the objective is to learn a function,  $V$  (the value function is usually denoted as  $Q$ , but we change this to  $V$  to avoid confusion with the code rate), from observations of the environment to approximate the action-value function  $V_{\mathcal{F}}$ . Then, given the estimated action-value function,  $V$ , and a state,  $\mathbf{h}_t$ , actions are selected as

$$a_t = \arg \max_{a \in \mathcal{A}} V(\mathbf{h}_t, a). \quad (16)$$

The state transitions in the MDP are complex, as they depend both on the transmission of the new codeword symbols and the BP decoder, so we cannot model them analytically. Additionally, since  $\mathcal{S} = [0, \log_2 q]^{L_0}$ , the state space is infinite, so using a lookup table would not be feasible [26]. Instead, we consider the DQN approach [24], which uses a neural network to approximate the value function.

### B. Deep Q-Learning

The DQN takes the state of the system, i.e., the entropy vector  $\mathbf{h}_t$  defined in Eq. (8), as input, and returns an estimate of the expected termination reward for each possible action, i.e.,  $V(\mathbf{h}_t, a_t)$ ,  $\forall a_t \in \mathcal{A}$ . We parameterize the function  $V$  as a fully connected deep neural network with number of layers and number of hidden units in the respective layers expressed by the list  $N_{\text{hidden}}$ . In each of the hidden layers, a rectified linear unit (ReLU) is used as the activation function and the output layer has  $L_0$  units.

In order to train the neural network, we adopt the replay memory approach from [24], in which the environment is simulated and the agent experience is stored in tuples  $e_t = (\mathbf{h}_t, a_t, r_t, \mathbf{h}_{t+1})$ . The replay memory buffer size is denoted by MEM, and as new experience samples are observed the oldest experience is deleted from the replay memory buffer. During training, batches of size BS are sampled from the replay memory in order to optimize the neural network parameters using backpropagation with the ADAM algorithm and gradient clipping with max gradient norm, GC.

The number of episodes between training sessions is  $F_{\text{upd}}$  and the number of parameter updating steps per training session is  $N_{\text{upd}}$ .

Moreover, as in [24], to avoid biases, two different  $V$  functions, denoted by  $V_A$  and  $V_B$ , are used to select and evaluate actions, respectively. The model is updated using the rule

$$V_A^{\text{new}}(\mathbf{h}_t, a_t) = (1 - \eta)V_A(\mathbf{h}_t, a_t) + \eta(r_t + \gamma_{\text{DQN}} \max_{a_{t+1} \in \mathcal{A}} V_B(\mathbf{h}_{t+1}, a_{t+1})), \quad (17)$$

where  $\eta$  is the learning rate and  $\gamma_{\text{DQN}}$  is the DQN discount factor. When  $\gamma_{\text{DQN}} = 0$ , the agent will strive to achieve immediate rewards while when  $\gamma_{\text{DQN}} = 1$ , the agent evaluates the actions based on the sum total of the future rewards. The parameters of  $V_B$  are then updated by copying the parameters of  $V_A$  after every  $F_{\text{mod}}$  training sessions.

During experience gathering, the agent uses the  $\varepsilon$ -greedy policy. The  $\varepsilon$ -greedy parameter is initialized as  $\varepsilon_0$  and decreases linearly with a decay parameter  $\varepsilon_d$  every  $F_\varepsilon$  simulated episodes, with a minimum preset as  $\varepsilon_{\text{min}}$ .

#### IV. SIMULATION SETTINGS AND RESULTS

We define a scenario corresponding to the one given in Sec. II, with a transmitter encoding packets containing  $K = 40$  bits of information into  $L_0 = 15$  symbols using a codebook of order  $q = 256$ , i.e., with code rate  $1/3$ . In the following, we will consider a modulation order of  $M = 256$  unless otherwise stated. Although this setting is more suitable for complex applications than for IoT [27], it simplifies the presentation: with this value, each codeword symbol maps exactly to one constellation point, i.e.,  $\hat{L}_t = L_t$ . We will also show results for quadrature phase-shift keying (QPSK) ( $M = 4$ ) below. We consider three baseline policies as benchmarks:

- 1) *HARQ*: we fix  $L_t$  to a constant for each  $t > 0$  and use a random uniform symbol selection policy to select  $L_t$  different symbols. This policy only requires 1 bit of feedback as with traditional HARQ. We set  $L_f = 1$ , i.e., feedback coded into 8 bits.
- 2) *Static tapered (ST) HARQ*: we fix  $L_t$  to a constant for each  $t > 0$ . Unlike the HARQ policy, this policy selects the maximum entropy symbols using Eq. (8); hence, for the first round the full 15 bit feedback is required. We set  $L_f = 2$ , i.e., feedback coded into 16 bits.
- 3) *Threshold-based adaptive (TA) HARQ*: this policy selects for retransmission all the symbols that have an entropy higher than a given threshold value  $H_{\text{th}}$ , hence, it requires the full 15 bit feedback. Again, we set  $L_f = 2$ , i.e., feedback coded into 16 bits.

TABLE I  
SCENARIO AND DQN SETTINGS

Parameter	Value	Description	Parameter	Value	Description
$K$	40 bits	Payload size	$L_0$	15 symbols	Codeword length
$q$	256	Galois field order	SNR	6 dB	Received SNR
$I$	5	Max BP iterations	$E_{\text{first}}$	0.6 mJ	Energy reference [28]
$\tau_p$	1 ms	Packet slot duration	$\mathbb{E}_{\mathcal{F}_0}[T]$	7.7	Reward normalization factor
$T_{\text{max}}$	15	Max (re)transmission rounds	$\eta$	0.001	Learning rate
BS	64	Batch size	$F_{\text{upd}}$	100	Training frequency
GC	5	Max gradient norm	MEM	60000	Memory replay buffer
$N_{\text{upd}}$	15	Training steps per update	$N_{\text{hidden}}$	[64, 32, 16]	Hidden layer sizes
$F_{\text{mod}}$	10	Target update frequency	$\varepsilon_d$	0.05	Exploration decay rate
$\varepsilon_0$	1	Initial exploration rate	$F_\varepsilon$	8000	Exploration decay frequency
$\varepsilon_{\text{min}}$	0.4	Min exploration rate	$N_{\text{test}}$	30000	Test episodes
$N_{\text{train}}$	270000	Training episodes			

In this study, for  $L_p = 0$  the energy cost of the first round is fixed as  $E_{\text{first}} = 0.6$  mJ, and a constant packet transmission slot of  $\tau_p = 1$  ms is set. These values are consistent with empirical measurements for LoRa deployments [28]. Moreover, we consider a maximum number of  $T_{\text{max}} = 15$  (re)transmissions. Finally, the baseline policy used for normalization,  $\mathcal{F}_0$ , is chosen as the ST policy with  $L_t = 1$ ,  $\forall t > 0$ . Then, the reward function defined in Eq. (11) simplifies as

$$r_T = (2 \cdot \mathbb{1}[\hat{\mathbf{c}}_T = \mathbf{c}] - 1) - \frac{1}{(P_s + E_o) \mathbb{E}_{\mathcal{F}_0}[T]} \sum_{t=1}^T E(t). \quad (18)$$

All parameters for the DQN architecture and training, as well as the simulation scenario, are given in Table I.

For the numerical experiments, we first consider a static AWGN channel with an SNR of 6 dB. For this special case, we first show the hyperparameter optimization of the baseline policies, then we analyze the influence of the discount factor and the energy model settings on the choices made by RAF, and finally RAF is compared to the optimized baselines for different energy model settings. Afterwards, two other scenarios are considered: (i) QPSK modulation with an AWGN channel, and (ii) 256-QAM modulation with a block fading channel where  $\beta_t \sim \mathcal{CN}(0, 1)$  are

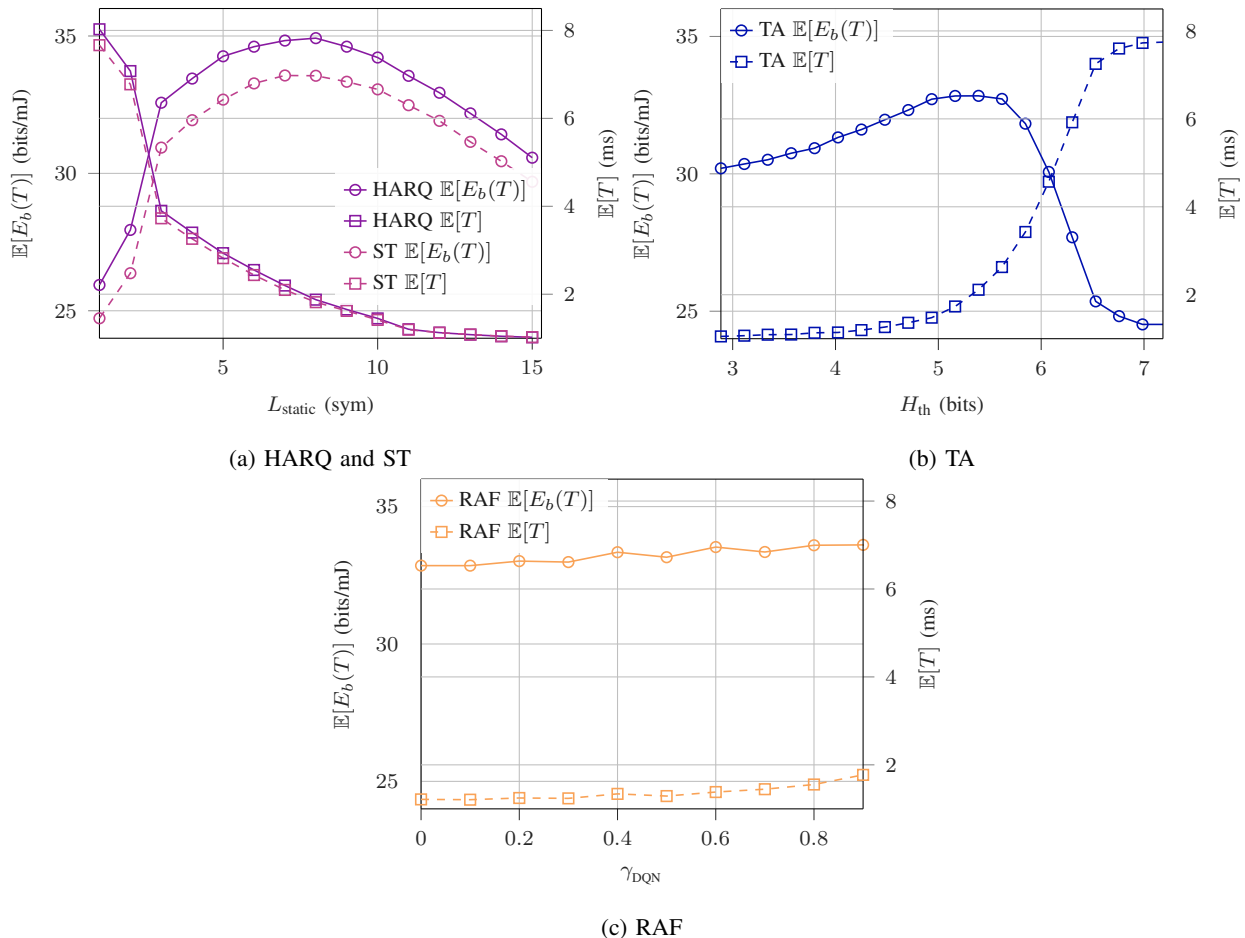


Fig. 3. Performance of the four policies HARQ, ST, TA, and RAF in terms of the average number of successfully transmitted bits per mJ and average latency when  $\alpha = 0.5$  and  $L_p = 1$  as a function of their respective parameters:  $L_{\text{static}}$  for HARQ and ST, the entropy threshold  $H_{\text{th}}$  for TA, and the discount factor  $\gamma_{\text{DQN}}$  for RAF.

independent and identically distributed (iid.). For the three aforementioned scenarios, the Pareto dominance of the proposed RAF scheme is shown.

### A. Hyperparameter Optimization

Given the transmission protocol specification  $L_p$ , the hardware specification  $\alpha$ , and the desired energy-latency trade-off through the exponential discount factor  $\gamma$ , we can optimize hyperparameters for the baseline policies and RAF.

We first consider the optimization of the baseline policies by grid search: For the TA policy, the only parameter is  $H_{\text{th}}$  while for the static policies the parameters are  $L_t \in \mathcal{A}$  for  $t = 1, \dots, T_{\text{max}} - 1$ . Due to the relatively large number of parameters for the static baselines, a



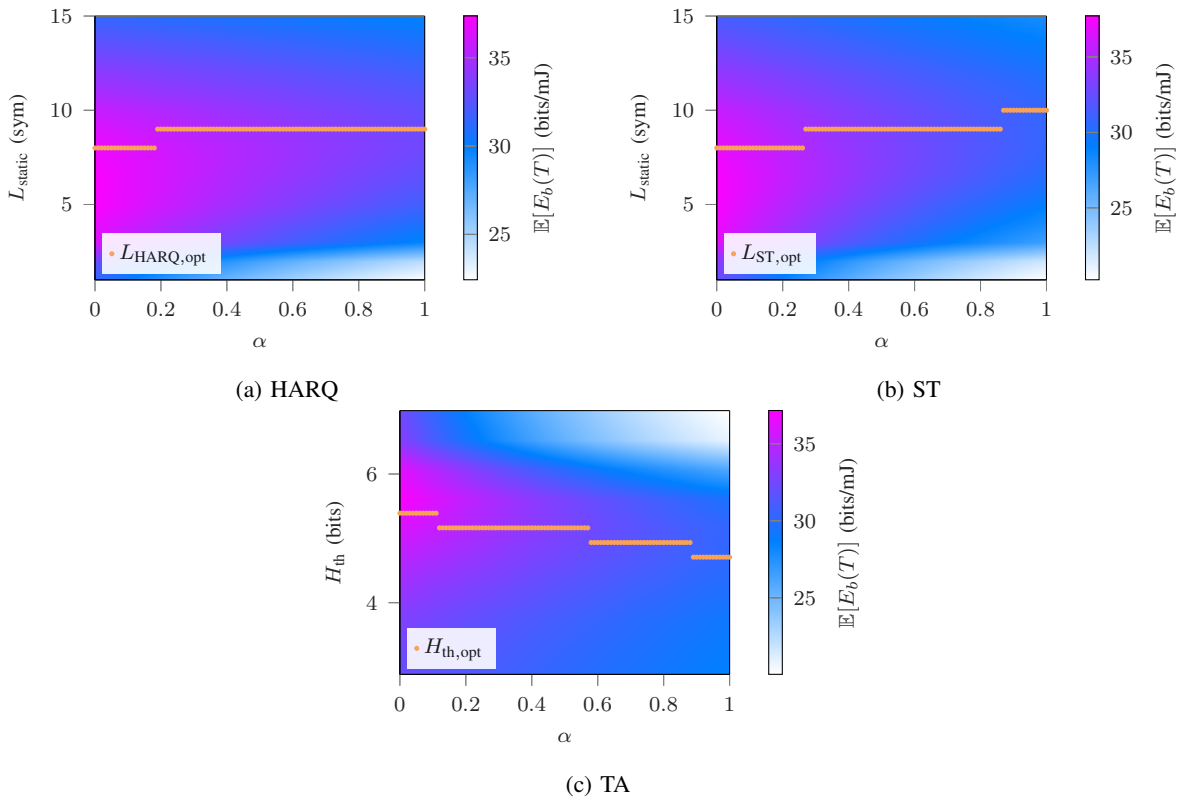


Fig. 4. Average number of successfully transmitted bits per energy  $E_b$  for the baseline policies as a function of  $\alpha$  and their respective parameters with  $L_p = 1$  and  $\gamma = 0.95$ .

grid search is infeasible. Instead, the sequence  $L_t$  is defined in terms of a single parameter  $L_{\text{static}} \in \{1, \dots, L_0\}$  as

$$L_t = \begin{cases} L_{\text{static}} & \text{if } t = 1, \\ 1 & \text{if } L_{\text{static}} \leq 2 \wedge t > 1, \\ 2 & \text{if } 2 < L_{\text{static}} \leq 10 \wedge t > 1, \\ 4 & \text{if } 10 < L_{\text{static}} \wedge t > 1, \end{cases} \quad (19)$$

where this definition is motivated by empirical results indicating that the optimal policy tends to be tapered. With this definition, we can do a grid search for the static baselines in terms of the single parameter  $L_{\text{static}}$ .

Figs. 3a-b show the performance of the baseline policies when  $L_p = 1$  and  $\alpha = 0.5$  in terms of the average number of successfully transmitted bits per mJ, defined as  $\mathbb{E}[E_b(T)]$  (bits/mJ), and average latency, defined as  $\mathbb{E}[T]$  (ms). It is observed that as  $L_{\text{static}}$  increases or as  $H_{\text{th}}$  decreases, the latency decreases, however, the energy-efficiency is unimodal. Hence, when  $\gamma = 1$ , the

parameter maximizing  $\mathbb{E}[E_b(T)\gamma^T]$  for HARQ is  $L_{\text{HARQ,opt}} = 8$ , for ST it is  $L_{\text{ST,opt}} = 7$ , and for TA it is  $H_{\text{th,opt}} = 5.39$ . Then, as  $\gamma$  decreases, the optimal parameters for the static baselines increase while for TA it decreases, in order to yield a lower latency.

The dependency of the optimal hyperparameters for the baseline policies on  $\alpha$  is shown in Figs. 4a-c: as the  $\alpha$  parameter decreases, it becomes increasingly expensive to retransmit symbols with respect to receiving feedback, and the optimal hyperparameters for the static baselines increases while the threshold for TA decreases. Notably, lower values of  $\alpha$  will also lead to higher latencies, as the number of retransmission rounds increases. A similar observation can be made for the preamble length  $L_p$ . Hence, the trade-off between energy-efficiency and latency is controlled both by the two physical parameters  $\alpha$  and  $L_p$ , and the discount factor  $\gamma$ .

The RAF policy has many hyperparameters, as seen from Table I. However, the parameters defining the energy-latency trade-off in the reward scheme defined in Eq. (18), i.e.,  $\alpha$  and  $L_p$ , and the discount factor for DQN updates used in Eq. (17), i.e.,  $\gamma_{\text{DQN}}$ , are particularly important. The rest of the hyperparameters for the neural network, neural network training, and RL exploration have been selected based on preliminary tests.

The influence of the discount factor  $\gamma_{\text{DQN}}$  on the energy-latency trade-off for RAF is shown in Fig. 3c: as  $\gamma_{\text{DQN}}$  increases, the RL agent is trained to be more foresighted, resulting in more energy-efficient actions, at the cost of higher latency. However, the differences in energy-efficiency and latency when varying the discount factor are relatively small.

### B. Adaptivity of RAF

Fig. 5 provides a better intuition for the choices made by the RAF scheme. The figures on the left depict colormaps representing the empirical probability density function (EPDF) of the chosen actions defined as

$$p_{\text{action}}^t(a) \triangleq \frac{1}{N_{\text{test}}} \sum_{j=1}^{N_{\text{test}}} \mathbb{1}[a_{t,j} = a], \quad (20)$$

where  $a_{t,j} \in \mathcal{A}$  is the action taking in the  $t$ -th round of the  $j$ -th episode. We can notice that the strategy is generally tapered, i.e., more symbols are retransmitted in the first few rounds, and that higher values of  $\alpha$  correspond to fewer retransmitted symbols per round and more rounds. The figures on the right show the EPDF of the minimum entropy among the transmitted symbols

in the first few rounds (i.e., the optimal entropy threshold, which we denote by  $H_{\min}(t)$  for the  $t$ -th round) defined as

$$p_{\text{entropy}}^t(h) \triangleq \frac{1}{|I_1^t| \sum_{j=1}^{N_{\text{test}}} \mathbb{1}[t \leq T_j]} \sum_{j=1}^{N_{\text{test}}} \sum_{i=1}^{I_{\text{max}}} \mathbb{1}[H_{\min,j}(t) \in I_i^t \wedge h \in I_i^t], \quad (21)$$

where  $\{I_i^t\}_{i=1}^{I_{\text{max}}}$  is a disjoint partition of  $[\min(\{H_{\min,j}(t)\}_j), \max(\{H_{\min,j}(t)\}_j)]$  into  $I_{\text{max}}$  intervals of equal Lebesgue measure,  $|\cdot|$  is the Lebesgue measure,  $T_j$  is the number of rounds in the  $j$ -th episode, and  $H_{\min,j}(t)$  is the minimum entropy among transmitted symbols in the  $t$ -th round of the  $j$ -th episode. Interestingly, the entropy distribution changes significantly from the first to the second round, but only slightly in subsequent rounds: this is due to the limited amount of information delivered in shorter retransmitted packets. Finally, we note that the distribution of the minimum entropy among the transmitted symbols has a high variance, as the fading and noise realizations might result in significantly different confidence levels at the decoder output: the optimal action is then hard to capture with a fixed threshold, making the TA policy highly suboptimal.

We note that the same results have been observed when fixing  $\alpha$  and varying  $\gamma_{\text{DQN}}$ , although changes in  $\alpha$  results in larger changes to the “aggressiveness” of the policy than  $\gamma_{\text{DQN}}$ .

### C. Comparison of Optimized Policies

Let us consider the performance of RAF when  $L_p = 1$ , trained with different values of  $\alpha$ : Fig. 6 shows the average performance for the various policies in terms of latency, successful bits per mJ, and undetected error rate (UDER), defined as  $\mathbb{E}[\mathbb{1}[\hat{c}_T \neq c]]$ . For each policy,  $\mathbb{E}[E_b(T)\gamma^T]$  with  $\gamma = 0.92$  is maximized according to the respective parameters:  $L_{\text{static}}$ ,  $H_{\text{th}}$ , and  $\gamma_{\text{DQN}}$ . Figs. 6a-b show that RAF can outperform HARQ in terms of the number of successfully transmitted bits for the same energy for lower values of  $\alpha$ , while also maintaining a lower latency. Additionally, TA has the worst overall performance in terms of the number of successfully transmitted bits per energy unit, and while ST has a slightly lower latency than HARQ, for larger values of  $\alpha$  the cost of rich feedback makes HARQ the preferred baseline policy. Finally, we look at the UDER, shown in Fig. 6c, from which we note that HARQ tends to have the most undetected errors. This highlights another critical advantage of rich feedback: retransmitting the highest-entropy symbols can steer the BP decoder towards the right codeword, reducing undetected errors. However, we note that the estimates of the undetected error rates are subject to significant variance since the occurrence of undetected errors are extreme observations.

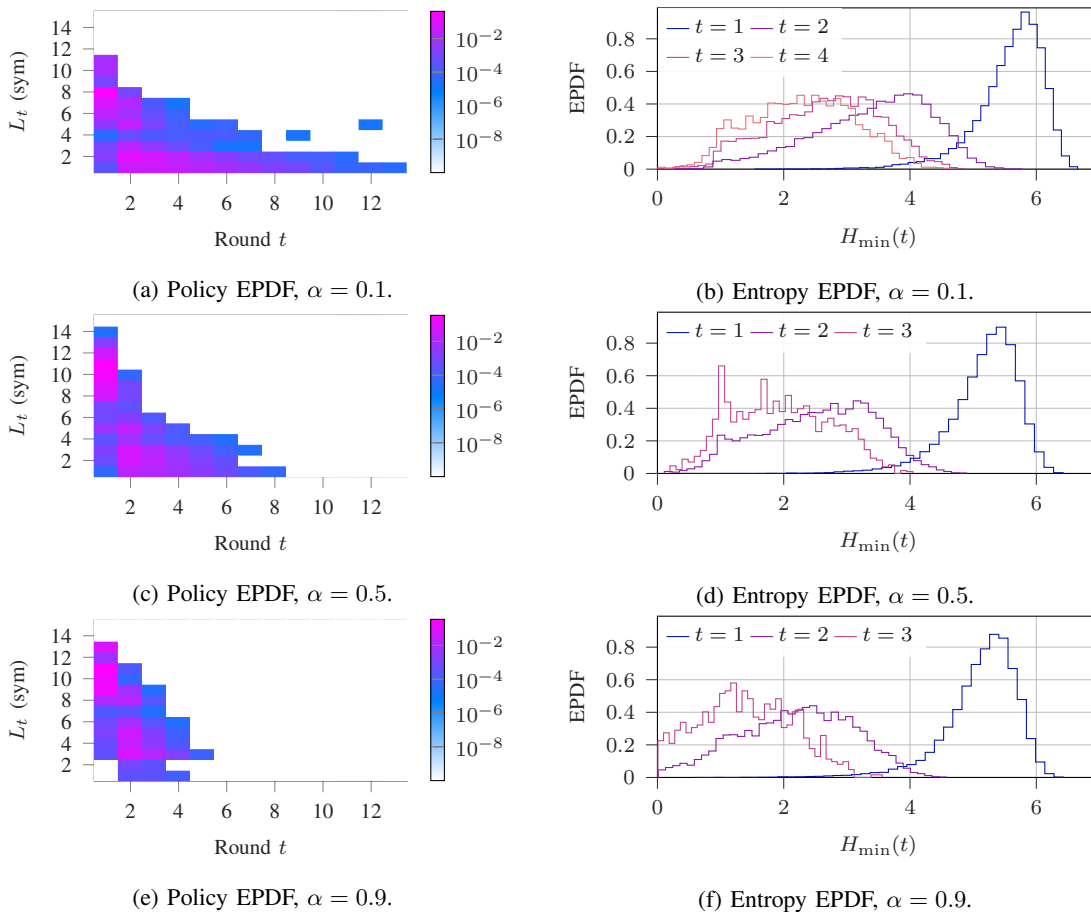


Fig. 5. Colormaps showing the EPDF of chosen actions (left) and  $H_{\min}$  (right) with RAF for  $L_p = 1$  and  $\gamma_{\text{BQ}} = 0.5$ .

Table II shows the average latency and energy-efficiency for  $\alpha \in \{0.1, 0.5, 0.9\}$ , with boldface indicating the best value in each row. It is seen that RAF is the most energy efficient policy when  $\alpha = 0.1$  while having a lower latency than the static baselines resulting in the best performance for the energy-latency trade-off. Specifically, when comparing RAF with HARQ with  $\alpha = 0.1$  and  $\gamma = 0.92$ , we are able to reduce the error rate by one third, while also reducing the latency by 3.8 percent and increasing the energy-efficiency by 0.39 percent. However, for higher  $\alpha$ -values, the cost of feedback outweighs the benefits of RAF and HARQ becomes the best policy.

#### D. Pareto Dominance of RAF

In order to properly compare the performances, we need to consider both the latency and the energy-efficiency. We evaluate them via the *Pareto frontier* for  $\alpha = 0.1$ , since RAF is convenient when receiving feedback consumes less energy than transmitting. Let  $\mathcal{K}$  be the set of feasible configurations for a specific scheme and  $f : \mathcal{K} \rightarrow \mathbb{R}^2$  be a mapping from the space of feasible

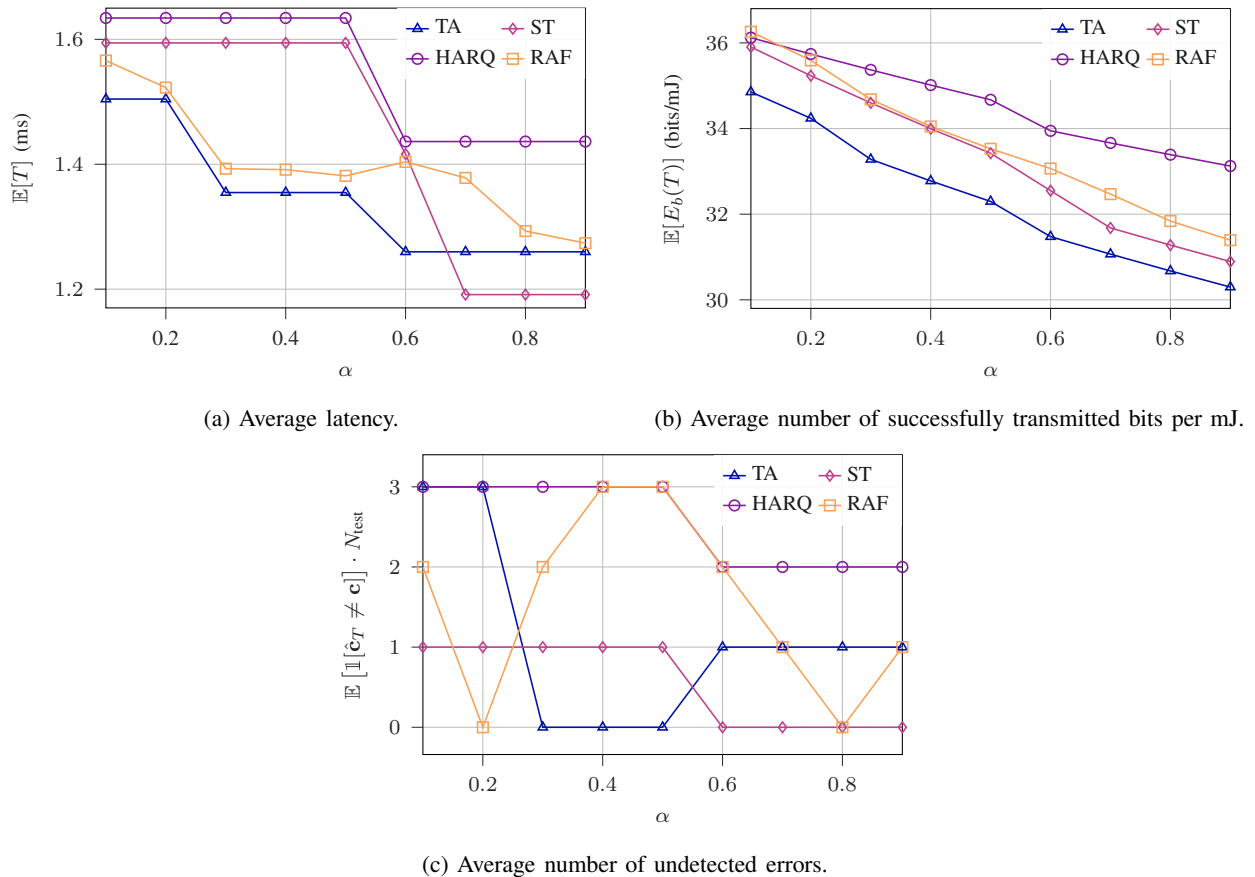
Fig. 6. KPIs as a function of  $\alpha$  with  $L_p = 1$ .

TABLE II  
COMPARISON OF RAF WITH THE BASELINE METHODS

Scheme	$\mathbb{E}[T]$ (ms)			$\mathbb{E}[E_b(T)]$ (bits/mJ)			$\mathbb{E}[E_b(T)\gamma^T]$		
	$\alpha=0.1$	$\alpha=0.5$	$\alpha=0.9$	$\alpha=0.1$	$\alpha=0.5$	$\alpha=0.9$	$\alpha=0.1$	$\alpha=0.5$	$\alpha=0.9$
HARQ	1.63	1.63	1.44	36.12	<b>34.67</b>	<b>33.12</b>	31.98	<b>30.74</b>	<b>29.73</b>
ST	1.59	1.59	<b>1.19</b>	35.90	33.42	30.89	31.84	29.69	28.12
TA	<b>1.50</b>	<b>1.35</b>	1.26	34.85	32.30	30.30	31.20	29.16	27.63
RAF	1.57	1.38	1.27	<b>36.26</b>	33.53	31.39	<b>32.20</b>	30.13	28.42

configurations to an energy-efficiency and latency value. Next, let  $\mathcal{Y} = \{(E, T) : (E, T) = f(k), k \in \mathcal{K}\}$ , where  $E$  is the energy-efficiency and  $T$  is the average latency. The *Pareto frontier* is the set

$$\mathcal{P}(\mathcal{Y}) = \{(E, T) \in \mathcal{Y} : \forall (E', T') \in \mathcal{Y} : E \geq E' \vee T \leq T'\}.$$

The Pareto region is then the set of points whose performance is worse than the ones on the frontier, and a policy *Pareto dominates* another if the Pareto frontier for the latter is contained in the former's Pareto region. The feasible configurations are defined through the tested hyperparameter settings. These values are  $L_{\text{static}} = 1, 2, \dots, 15$  for HARQ and ST,  $H_{\text{th}} = 2.9, 3.1, \dots, 7.1$  for TA, and  $\gamma_{\text{DQN}} = 0.1, 0.2, \dots, 0.9$ ,  $\alpha = 0.1, 0.5$ , and  $L_p = 1, 2$  for RAF.

Figs. 7a and 7b depict the Pareto frontiers when  $\alpha = 0.1$  and  $L_p = 1, 2$  for the average number of successfully transmitted bits per energy unit versus the average latency (in ms) for the baselines and the RAF model. These results show that RAF Pareto dominates the baselines for both preamble lengths, achieving a significantly lower latency for the same energy-efficiency (or, conversely, a higher energy-efficiency with the same latency).

Until now, we have only considered an AWGN channel and 256-QAM modulation. However, the RAF model can be adapted to different modulation schemes and other channels. To illustrate this, the baseline policies and the RAF model have been tested with QPSK modulation with an AWGN channel and 256-QAM modulation with a block fading channel.

The QPSK modulation scheme is adapted to the 256-ary QAM symbols treated in this paper by mapping an order 256 GF value over four QPSK symbols, where each of the QPSK symbols has normalized energy. Due to the increased transmission power, and since a lower constellation order gives a more noise-resilient modulation, the SNR is also lowered to  $-3$  dB in order to obtain results that are comparable to the 256-QAM modulation. The results are shown in Figs. 7c and 7d: the RAF model can adapt to the modulation scheme, yielding Pareto dominant results for both of the considered modulation schemes.

The block fading channel assumes that  $\mathbf{y}_t = \beta_t \mathbf{x}_t + \mathbf{w}_t$ , where the fading coefficients  $\beta_t \sim \mathcal{CN}(0, 1)$  are iid.. The instantaneous SNR is then  $\text{SNR}_t = \frac{|\beta_t|^2}{\sigma^2}$ , with a mean SNR set to 6 dB. In these experiments, the RAF models trained on the AWGN channel are used for testing with the fading channel. The Pareto frontiers are seen in Figs. 7e and 7f. We can draw two conclusions from these figures: firstly, the static policies cannot adapt to a fading channel since the decisions made by the agents are independent of the instantaneous channel, hence, the TA policy is the best baseline policy, and secondly, the RAF model can generalize to a fading channel while maintaining Pareto dominance.

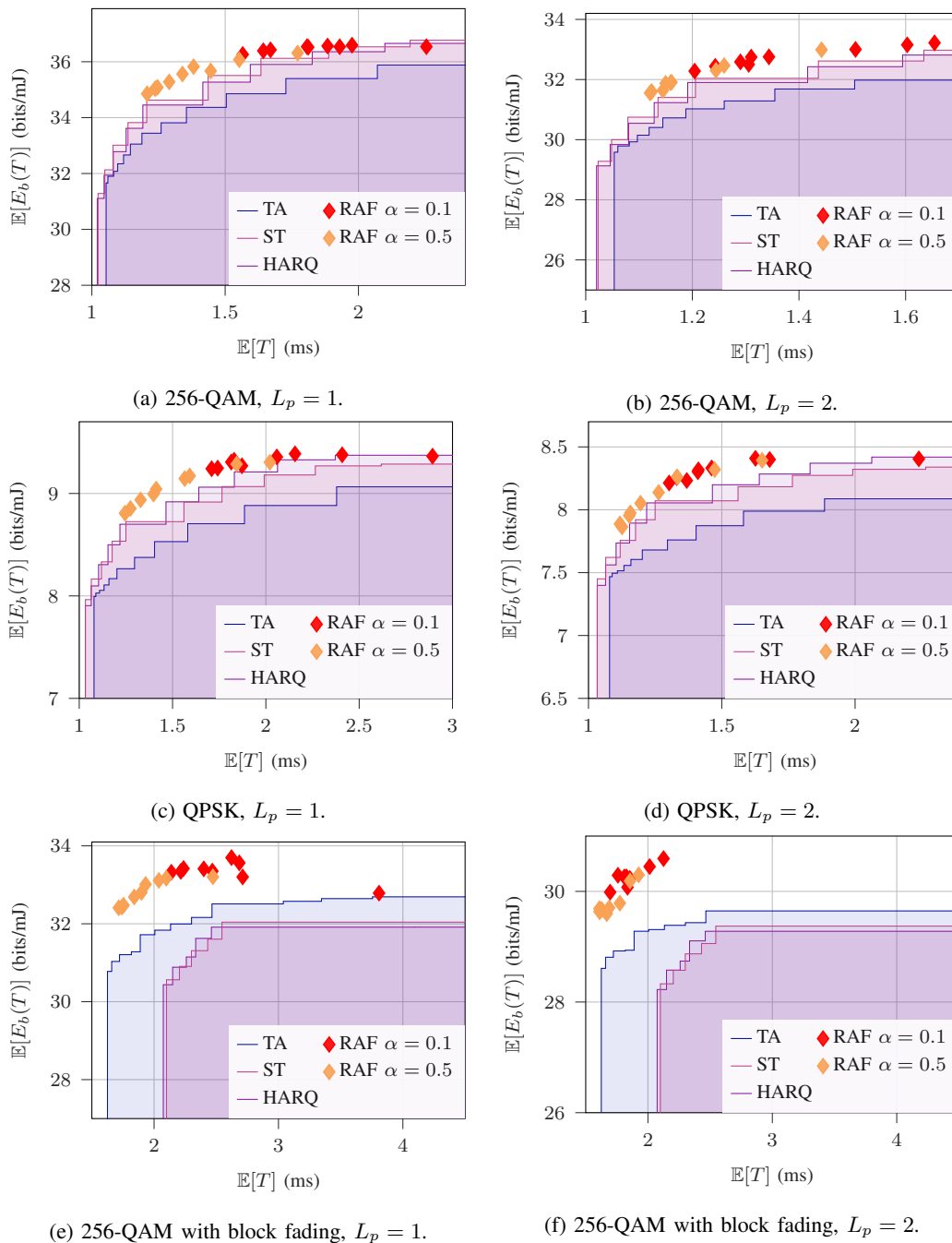


Fig. 7. Pareto frontiers for the average successful bits per mJ versus the average latency in ms for the different baselines and the RAF model when  $\alpha = 0.1$  and  $L_p = 1, 2$ .

## V. CONCLUSIONS AND FUTURE WORK

In this work, we presented RAF, a DQN-based scheme that can improve HARQ performance for short-packet transmissions by energy-conscious devices. The scheme moves the complexity of adaptive HARQ to the receiver side, whose energy constraints are significantly looser: the

battery-limited transmitter only needs to decode the rich feedback and retransmit the requested symbols, while all decisions are made by the receiver. We considered different relative costs for transmitting and receiving feedback, based on state of the art energy models, as well as different preamble lengths, and show that rich feedback with a relatively high feedback cost achieves Pareto dominant policies in the energy efficiency-latency trade-off. The Pareto dominance of RAF was highlighted for both 256-QAM and QPSK modulation schemes with an AWGN channel as well as a block fading channel. Furthermore, we showed that the rich feedback proposed in this work achieves a lower risk of undetected errors.

In future work, we aim at refining the scheme further, considering more complex channels whose statistics can be learned and exploited by the receiver to further optimize the HARQ process, as well as more complex energy models.

## REFERENCES

- [1] F. Zhou and Y. Chai, "Near-sensor and in-sensor computing," *Nat. Electron.*, vol. 3, no. 11, pp. 664–671, 2020.
- [2] F. Guo, F. R. Yu, H. Zhang, X. Li, H. Ji, and V. C. M. Leung, "Enabling massive IoT toward 6G: A comprehensive survey," *IEEE Internet Things J.*, vol. 8, no. 15, pp. 11 891–11 915, 2021.
- [3] R. K. Singh, P. P. Puluckul, R. Berkvens, and M. Weyn, "Energy consumption analysis of LPWAN technologies and lifetime estimation for IoT application," *Sensors*, vol. 20, no. 17, p. 4794, 2020.
- [4] K. Mekki, E. Bajic, F. Chaxel, and F. Meyer, "A comparative study of LPWAN technologies for large-scale IoT deployment," *ICT Express*, vol. 5, no. 1, 2019.
- [5] A. Ahmed, A. Al-Dweik, Y. Iraqi, H. Mukhtar, M. Naeem, and E. Hossain, "Hybrid automatic repeat request (HARQ) in wireless communications systems and standards: A contemporary survey," *IEEE Commun. Surv. Tutor.*, vol. 23, no. 4, pp. 2711–2752, 2021.
- [6] H. Farès, B. Vrigneau, and O. Berder, "Green communication via HARQ protocols using message-passing decoder over AWGN channels," in *26th Annu. Int. Symp. Pers., Indoor, and Mobile Radio Commun. (PIMRC)*. IEEE, 2015, pp. 197–201.
- [7] A. Avranas, M. Kountouris, and P. Ciblat, "Energy-latency tradeoff in ultra-reliable low-latency communication with retransmissions," *IEEE J. Sel. Areas Commun. (JSAC)*, vol. 36, no. 11, pp. 2475–2485, 2018.
- [8] P. Andres-Maldonado, M. Lauridsen, P. Ameigeiras, and J. M. Lopez-Soler, "Analytical modeling and experimental validation of NB-IoT device energy consumption," *IEEE Internet Things J.*, vol. 6, no. 3, pp. 5691–5701, 2019.
- [9] F. Li, H. Yao, J. Du, C. Jiang, and F. R. Yu, "Green communication and computation offloading in ultra-dense networks," in *IEEE Global Telecommun. Conf. (GLOBECOM)*, 2019.
- [10] Y.-P. E. Wang, X. Lin, A. Adhikary, A. Grovlen, Y. Sui, Y. Blankenship, J. Bergman, and H. S. Razaghi, "A primer on 3GPP narrowband internet of things," *IEEE Commun. Mag.*, vol. 55, no. 3, pp. 117–123, 2017.
- [11] R. Wesel, N. Wong, A. Baldauf, A. Belhouchat, A. Heidarzadeh, and J.-F. Chamberland, "Transmission lengths that maximize throughput of variable-length coding & ACK/NACK feedback," in *IEEE Global Telecommun. Conf. (GLOBECOM)*, 2018.



- [12] H. Yang, R. C. Yavas, V. Kostina, and R. D. Wesel, "Variable-length stop-feedback codes with finite optimal decoding times for BI-AWGN channels," in *Int. Symp. Inf. Theory (ISIT)*. IEEE, 2022, pp. 2327–2332.
- [13] S. Pfletschinger, D. Declercq, and M. Navarro, "Adaptive HARQ with non-binary repetition coding," *IEEE Trans. Wirel.*, vol. 13, no. 8, pp. 4193–4204, 2014.
- [14] L. Szczecinski, S. R. Khosravirad *et al.*, "Rate allocation and adaptation for incremental redundancy truncated HARQ," *IEEE Trans. Commun. (TCOM)*, vol. 61, no. 6, pp. 2580–2590, 2013.
- [15] S. K. Ankireddy, S. A. Hebbbar, Y. Jiang, H. Kim, and P. Viswanath, "Compressed error HARQ: Feedback communication on noise-asymmetric channels," *arXiv preprint arXiv:2302.10170*, 2023.
- [16] C.-W. Hsu, A. Anastasopoulos, and H.-S. Kim, "Instantaneous feedback-based opportunistic symbol length adaptation for reliable communication," *IEEE Trans. Commun. (TCOM)*, 2023.
- [17] Y. Jiang, H. Kim, H. Asnani, S. Oh, S. Kannan, and P. Viswanath, "Feedback turbo autoencoder," in *Int. Conf. Acoust., Speech and Signal Process. (ICASSP)*. IEEE, 2020, pp. 8559–8563.
- [18] E. Ozfatura, Y. Shao, A. G. Perotti, B. M. Popović, and D. Gündüz, "All you need is feedback: Communication with block attention feedback codes," *IEEE J. on Sel. Areas Inf. Theory (JSAIT)*, vol. 3, no. 3, pp. 587–602, 2022.
- [19] V. Ninkovic, D. Vukobratovic, C. Häger, H. Wymeersch *et al.*, "Rateless autoencoder codes: Trading off decoding delay and reliability," *arXiv preprint arXiv:2301.12231*, 2023.
- [20] M. Davey and D. MacKay, "Low density parity check codes over  $GF(q)$ ," *IEEE Commun. Lett.*, vol. 2, no. 6, pp. 70–71, 1998.
- [21] G. Durisi, G. Liva, and Y. Polyanskiy, "Short-Packet Transmission," in *Information Theoretic Perspectives on 5G Systems and Beyond*. Cambridge Univ. Press, 2020.
- [22] K. Kasai, D. Declercq, C. Poulliat, and K. Sakaniwa, "Multiplicatively repeated nonbinary LDPC codes," *IEEE Trans. Inf. Theory*, vol. 57, no. 10, pp. 6788–6795, 2011.
- [23] R. S. Sutton and A. G. Barto, *Reinforcement Learning: An Introduction*. A Bradford Book, 2018.
- [24] V. Mnih, K. Kavukcuoglu, D. Silver, A. A. Rusu, J. Veness, M. G. Bellemare, A. Graves, M. Riedmiller, A. K. Fidjeland, G. Ostrovski *et al.*, "Human-level control through deep reinforcement learning," *Nature*, vol. 518, no. 7540, pp. 529–533, 2015.
- [25] H. Sun, L. Han, R. Yang, X. Ma, J. Guo, and B. Zhou, "Optimistic curiosity exploration and conservative exploitation with linear reward shaping," *arXiv preprint arXiv:2209.07288*, 2022.
- [26] L. Baird, "Residual algorithms: Reinforcement learning with function approximation," in *Machine Learning Proceedings 1995*, A. Prieditis and S. Russell, Eds. Morgan Kaufmann, 1995, pp. 30–37.
- [27] P. K. Singya, P. Shaik, N. Kumar, V. Bhatia, and M.-S. Alouini, "A survey on higher-order QAM constellations: Technical challenges, recent advances, and future trends," *IEEE Open J. Commun. Soc. (OJ-COMS)*, vol. 2, pp. 617–655, 2021.
- [28] T. Bouguera, J.-F. Diouris, J.-J. Chaillout, R. Jaouadi, and G. Andrieux, "Energy consumption model for sensor nodes based on LoRa and LoRaWAN," *Sensors*, vol. 18, no. 7, p. 2104, 2018.